

PAPER • OPEN ACCESS

The influence of silicon on topographical parameters and mechanical properties of the Ti-Ni-Ta-Si surface alloy synthesized on the NiTi-substrates

To cite this article: F A D'yachenko *et al* 2021 *J. Phys.: Conf. Ser.* **1989** 012003

View the [article online](#) for updates and enhancements.

A promotional banner for the 240th ECS Meeting. The banner features a colorful striped border at the top. On the left, the ECS logo is displayed in a green circle. To its right, the text reads "240th ECS Meeting" in large blue font, followed by "Oct 10-14, 2021, Orlando, Florida" in a smaller blue font. Below this, it says "Register early and save up to 20% on registration costs" in bold black font, and "Early registration deadline Sep 13" in a smaller black font. At the bottom left, there is a red "REGISTER NOW" button. On the right side of the banner, there is a photograph of a diverse group of people in professional attire, smiling and clapping, suggesting a successful event or presentation.

ECS **240th ECS Meeting**
Oct 10-14, 2021, Orlando, Florida
**Register early and save
up to 20% on registration costs**
Early registration deadline Sep 13
REGISTER NOW

The influence of silicon on topographical parameters and mechanical properties of the Ti-Ni-Ta-Si surface alloy synthesized on the NiTi-substrates

F A D'yachenko¹, A A Atovullaeva², E V Yakovlev³ and L L Meisner¹

¹Institute of Strength Physics and Materials Science SB RAS, Tomsk, Russia

²National Research Tomsk State University, Tomsk, Russia

³Institute of High-Current Electronics SB RAS, Tomsk, Russia

E-mail: frozenonnetroll@mail.ru

Abstract. This work comprises a study of the effect of silicon on the topographical parameters and mechanical properties of the Ti-Ni-Ta-Si surface alloy (SA) synthesized on the NiTi-substrates by the additive thin-film electron-beam method. It was found that the roughness of [Ti-Ni-Ta-Si]SA ($\sim 0.095 \mu\text{m}$) has a lower value than in [Ti-Ni-Ta]SA ($\sim 0.195 \mu\text{m}$). The values of the yield strength σ_y in the surface layers of [Ti-Ni-Ta-Si]SA and [Ti-Ni-Ta]SA are characterized by a gradient decrease from ~ 4.2 GPa up to ~ 1.2 and ~ 1.7 GPa, respectively. During the indentation, evaluation of the deformation behavior (recovered elastic – ε_{elast} , and superelastic – ε_{SE} , residual plastic – ε_{plast} deformation) showed, that in surface layers of [Ti-Ni-Ta-Si]SA and [Ti-Ni-Ta]SA due to an increase of ε_{plast} , there was a decrease in ε_{SE} up to ~ 35 and $\sim 22\%$, respectively (for the NiTi-initial $\varepsilon_{SE} \approx 38\%$).

1. Introduction

The nickel titanium based alloys (NiTi) are known as smart materials that are capable to convert thermal energy into mechanical work [1]. Nowadays, these alloys are used to produce miniature devices (e.g., *actuators*) for the operation of the microelectromechanical systems (MEMS), which need to perform mechanical work under long-term dynamic alternating load. Considering that, the state of the surface of a miniature device has a great influence on its volume properties, it is necessary to modify the surface layers of NiTi alloys in order to improve their mechanical properties.

Low-energy high-current electron beam (LEHCEB) treatment is an effective way of modifying the surface layers of metallic materials [2, 3]. With addition of alloying elements, it allows producing a modified layer on the surface of miniature device without a sharp interface with the substrate material (such modified layer is called as a *surface alloy* (SA) [3-6]). The application of a LEHCEB treatment during the synthesis of a SAs has been successfully implemented for such systems as:

1) [Cr-film/Cu-substrate] [4], where an increase in the wear resistance of [Cr-Cu]SA was observed relative to the synthesized $\text{Cr}_{30}\text{Cu}_{70}$ (at. %) powder coatings;

2) the most relevant are the results of studies of the mechanical properties for SA based on the [Ni-film/Cu-substrate] system [6].

It is shown that the presence of SA makes it possible to get closer to the solution of the problem of the adhesive strength of coatings on the surface of metallic substrates formed by conventional methods (e.g., *PVD*-, *CVD-methods*).



Previously [5], the [Ti-Ni-Ta]SA and [Ti-Ni-Ta-Si]SA with a multiphase structure, a gradient of chemical composition, and mechanical properties were synthesized on the NiTi-substrates using the additive thin-film electron-beam method.

The studies in this work, carried out by the methods of optical metallography and optical interference profilometry, will make it possible to establish the effect of Si on the surface morphology and topographical parameters in systems [SA/NiTi-substrate]. Based on the results of the mechanical properties [5], the evaluation of the yield strength σ_y according to the [7] will expand the information of the elastic-plastic behavior of [Ti-Ni-Ta]SA and [Ti-Ni-Ta-Si]SA and determine the effect of Si on the mechanical properties in systems [SA/NiTi-substrate]. Here, investigating the [Ti-Ni-Ta]SA and [Ti-Ni-Ta-Si]SA on the NiTi-substrates, we study the influence of Si on the topographical parameters and mechanical properties in systems [SA/NiTi-substrate].

2. Experimental

2.1. Material

The material researched here is a commercial NiTi alloy (MATEK-SMA, Russia). The NiTi alloy has the following chemical composition: Ti (balance); 55.75 Ni; 0.035 O; 0.02 C; 0.003 N; 0.001 H (wt. %). The stages of the preliminary mechanical and physicochemical surface treatments before synthesis of [Ti-Ni-Ta]SA and [Ti-Ni-Ta-Si]SA on the NiTi-substrates were described in [8].

2.2. Additive thin-film electron-beam synthesis of [Ti-Ni-Ta]SA and [Ti-Ni-Ta-Si]SA

The synthesis of [Ti-Ni-Ta]SA was performed as follows. After preliminary LEHCEB treatment in the mode (i): the beam energy density $E_s = 3.8 \text{ J/cm}^2$, a pulse duration $\tau = 2.5 \text{ } \mu\text{s}$, the number of pulses $n = 32$; the NiTi-substrate was positioned by a manipulator along the magnetron sputter axis for deposition of $\text{Ti}_{70}\text{Ta}_{30}$ (here and below, at. %) film of $\sim 50 \text{ nm}$ thickness, and along the LEHCEB axis for pulsed melting of the [Ti-Ta-film/NiTi-substrate] system (at the mode $E_s = 2 \text{ J/cm}^2$, $n = 5$). The number of “deposition-melting” cycles was $N = 20$, so that the [Ti-Ni-Ta]SA was in total no thicker than $\sim 1 \text{ } \mu\text{m}$. The “deposition-melting” cycles on the modified automatic setup “RITM-SP” (Microsplyav, Russia) were performed in the single vacuum cycle [3].

In the same way, after preliminary LEHCEB treatment in the mode (ii): $E_s = 2.5 \text{ J/cm}^2$, $\tau = 2.5 \text{ } \mu\text{s}$, $n = 10$; the [Ti-Ni-Ta-Si]SA was synthesized on NiTi-substrate. The thickness of deposited $\text{Ti}_{60}\text{Ta}_{30}\text{Si}_{10}$ film was $\sim 100 \text{ nm}$. The pulsed LEHCEB melting of [Ti-Ta-Si-film/NiTi-substrate] system was: $E_s = 1.7 \text{ J/cm}^2$, $n = 10$. The number of “deposition-melting” cycles was $N = 10$, so that the [Ti-Ni-Ta-Si]SA was in total no thicker than $\sim 1 \text{ } \mu\text{m}$.

2.3. Methods of investigation

The study of the morphology of the surface was carried out by the method of optical metallography (OM) on the setup *Axiocvert 200MAT* (Zeiss, Germany) using the function of the differential interference contrast (DIC). The study of the topographical parameters was performed by the method of optical interference profilometry (OIP) on the setup *New View 6200* (Zygo, Germany).

The investigation of the mechanical properties and elastic-plastic behavior of [Ti-Ni-Ta]SA and [Ti-Ni-Ta-Si]SA on NiTi-substrates were examined by the method of instrumented indentation on the facilities: *Nano Hardness Tester* (CSM, Switzerland) and *NanoTest* (Micro Materials Ltd., Great Britain). The experimental conditions are described in detail [5, 8].

The evaluation of the yield strength σ_y is based on the model [7]. The deformation behavior of surface layers, that associated with the mechanisms of the formation and recovery of the imprint, was determined by the parameters ε_{plast} , ε_{SE} , ε_{elast} , which characterize the proportion of plastic deformation, and the recovery of superelastic and elastic deformation. The proportion of plastic deformation ε_{plast} was calculated by the formula:

$$\varepsilon_{plast} = \frac{h_r}{h_{max}} \times 100\% \quad (1)$$

where h_r – the residual indentation depth after unloading, h_{max} – maximum indentation depth under maximum load P_{max} .

The proportion of recovered superelastic deformation ε_{SE} was calculated by:

$$\varepsilon_{SE} = \frac{h_c - h_r}{h_{max}} \times 100\% \quad (2)$$

where h_c – the contact depth between the indenter and the specimen.

The proportion of recovered elastic deformation ε_{elast} was calculated by:

$$\varepsilon_{elast} = \frac{h_{max} - h_c}{h_{max}} \times 100\% \quad (3)$$

3. Experimental results and discussion

3.1. Morphology of surface of [Ti-Ni-Ta]SA and [Ti-Ni-Ta-Si]SA

Figure 1 shows optical (*a, b*) and 2D-digital (*c, d*) images of the surfaces obtained by the OM and OIP methods, respectively, as well as the profilograms of surfaces (*e, f*) in the directions indicated by the arrows on the 2D-images (*c, d*) for [Ti-Ni-Ta]SA (*a, c, e*) and [Ti-Ni-Ta-Si]SA (*b, d, f*). The surface of [Ti-Ni-Ta-Si]SA (figure 1*b*) is characterized by a less homogeneous microrelief as compared with [Ti-Ni-Ta]SA (figure 1*a*). Firstly, the resulting microrelief of the surface of [Ti-Ni-Ta-Si]SA is due to the mode of preliminary LEHCEB-treatment of NiTi-substrate ((ii) $E_s = 2.5 \text{ J/cm}^2$, $n = 10$). The NiTi-specimens before [Ti-Ni-Ta]SA synthesis were LEHCEB-treated by another mode ((i) $E_s = 3.8 \text{ J/cm}^2$, $n = 32$).

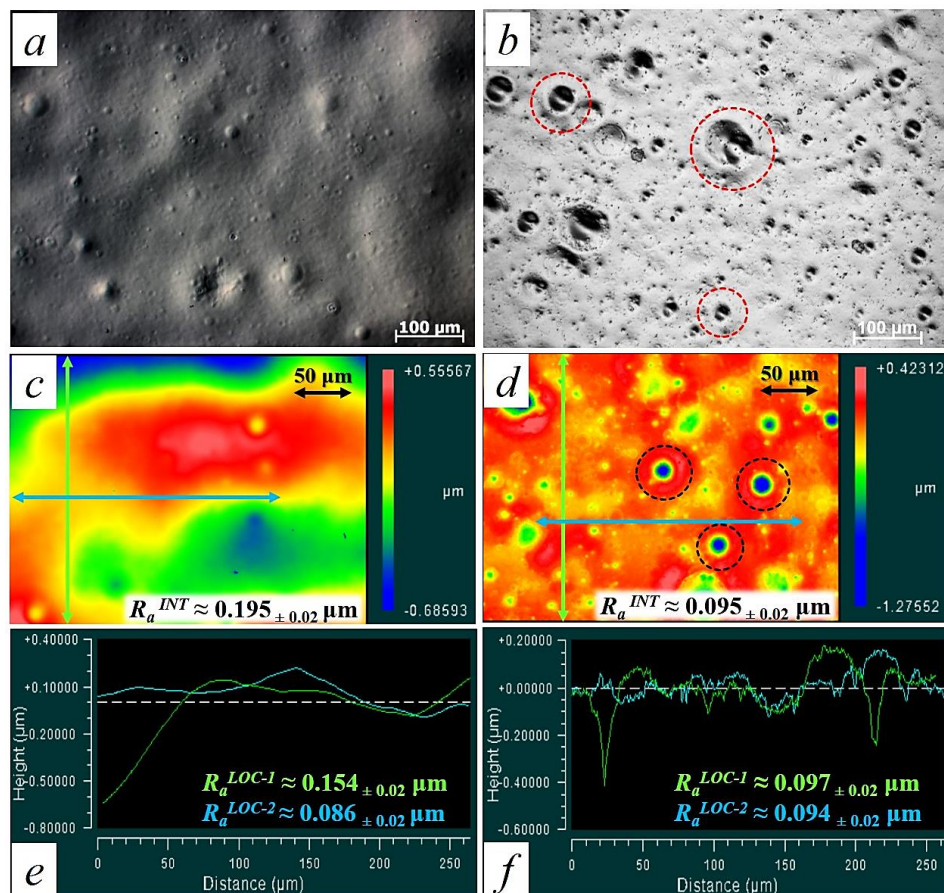


Figure 1. Optical DIC images (*a, b*), 2D-digital images (*c, d*), and profilograms of surface (*e, f*) of the [Ti-Ni-Ta]SA (*a, c, e*) and [Ti-Ni-Ta-Si]SA (*b, d, f*). On the figures (*c, d*) and (*e, f*) showed the values

of the integral parameter of roughness R_a^{INT} and local parameter of roughness R_a^{LOC-1} , R_a^{LOC-2} (the directions of profilograms showed on the figures (c, d))

Secondly, on the surface of the [Ti-Ni-Ta-Si]SA, there is a crater-like microrelief (figure 1b, marked by dotted circles). Unlike the [Ti-Ni-Ta]SA, during the synthesis of [Ti-Ni-Ta-Si]SA, the addition of Si₁₀ to the deposited Ti₆₀Ta₃₀Si₁₀ films led to the formation of [Ti-Ni-Ta-Si]SA, that has areas with a crater-like microrelief and with smoothed microrelief, which are homogeneously distributed over the surface of the specimen.

Figure 1d shows the investigations of the morphology and topography of the surface of NiTi-specimens with [Ti-Ni-Ta-Si]SA by the OIP method. It can be seen, that [Ti-Ni-Ta-Si]SA has areas with a crater-like and smooth microrelief, which were found in the optical images (figure 1b). A comparative analysis of the topographical parameters of surface between [Ti-Ni-Ta]SA and [Ti-Ni-Ta-Si]SA was carried out to determine the effect of silicon on the surface of SAs.

The profilogram of the [Ti-Ni-Ta]SA is characterized by a smooth surface (the value of the integral parameter of roughness $R_a^{INT} \approx 0.195 \mu\text{m}$, the local values along the orthogonal lines in the figure 1e are $R_a^{LOC-1} \approx 0.154 \mu\text{m}$ and $R_a^{LOC-2} \approx 0.086 \mu\text{m}$), with slight profile deviations in depth and height from $\sim 0.7 \mu\text{m}$ up to $\sim 0.6 \mu\text{m}$, respectively.

In the [Ti-Ni-Ta-Si]SA the value of the integral parameter of roughness decreases to $R_a^{INT} \approx 0.095 \mu\text{m}$ (figure 1f). The local values of the roughness along the lines in figure 1f are $R_a^{LOC-1} \approx 0.097 \mu\text{m}$ and $R_a^{LOC-2} \approx 0.094 \mu\text{m}$. As in [Ti-Ni-Ta]SA, in [Ti-Ni-Ta-Si]SA, the surface is smoothed, however, unlike [Ti-Ni-Ta]SA, on the [Ti-Ni-Ta-Si]SA surface observed areas with a crater-like microrelief (with diameter up to $\sim 60 \mu\text{m}$ (indicated in figure 1 (b, d)).

3.2. Yield strength in systems [SA/NiTi-substrate]

In [5], the studies of the strength and elastic-plastic properties in the specimens [Ti-Ni-Ta]SA and [Ti-Ni-Ta-Si]SA were carried out. It was shown that in the surface layers at a depth of $\sim 1 \mu\text{m}$ thickness in the [Ti-Ni-Ta]SA and [Ti-Ni-Ta-Si]SA, the dependences of the hardness H and Young's modulus E on the maximum indentation depth h_{max} have a gradient behavior. Figure 2 illustrates the dependences of the yield strength σ_y on the maximum indentation depth h_{max} at various values of the maximum load P_{max} on the indenter for NiTi-initial – curve 1, [Ti-Ni-Ta]SA – curve 2 and [Ti-Ni-Ta-Si]SA – curve 3. On the figure 2 dotted lines show the boundaries of the [Ti-Ni-Ta]SA ($\sim 1 \mu\text{m}$) and [Ti-Ni-Ta-Si]SA ($\sim 1.6 \mu\text{m}$), according to investigations of the structure of these SAs [5].

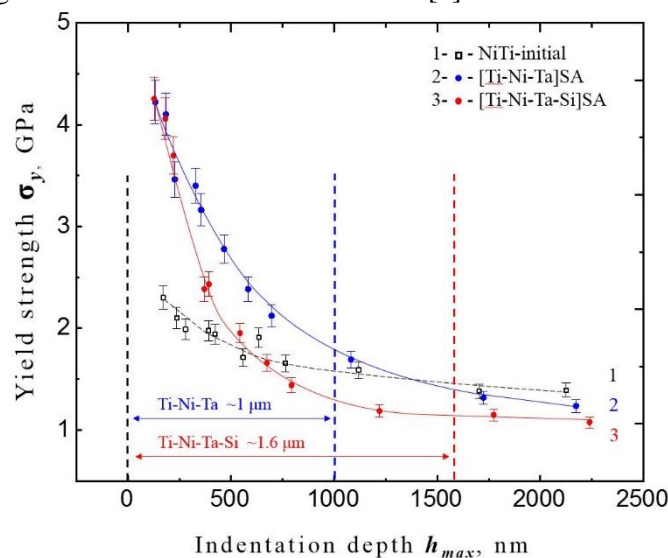


Figure 2. Dependences of the yield strength σ_y on the maximum indentation depth h_{max} : after preliminary mechanical and physicochemical surface treatments (NiTi-initial) – curve 1; [Ti-Ni-Ta]SA – curve 2; [Ti-Ni-Ta-Si]SA – curve 3. The dotted lines show the boundaries of synthesized SAs according to [5]

The yield strength σ_y of [Ti-Ni-Ta]SA and [Ti-Ni-Ta-Si]SA near the surface (at a depth of ~ 200 nm thickness) is ~ 4.2 GPa (figure 2, curves 2 and 3, respectively), for the NiTi-initial at a given depth $\sigma_y \approx 2.3$ GPa (figure 2, curve 1). In the layers of ~ 1 and ~ 1.6 μm thickness for [Ti-Ni-Ta]SA and [Ti-Ni-Ta-Si]SA, the values of σ_y smoothly decrease to ~ 1.7 and ~ 1.2 GPa, respectively. At a depth of more than ~ 2 μm thickness, the values of σ_y are close to NiTi-initial ($\sigma_y \approx 1.4$ GPa).

From the analysis of the dependences $H(h_{max})$, $E(h_{max})$ [5] and $\sigma_y(h_{max})$ (figure 2) for [Ti-Ni-Ta]SA and [Ti-Ni-Ta-Si]SA, the following correlation was found between the parameters H , E and σ_y . These parameters have similar values at small (up to ~ 250 nm thickness) and deep (from ~ 1300 nm thickness) indentation depths for both SAs. In the intermediate region (at a depth from ~ 250 up to ~ 1300 nm thickness), the correlation is not observed.

3.3. Evaluation of deformation behavior in systems [SA/NiTi-substrate]

Figure 3 shows the dependences of the behavior of the recovered elastic ϵ_{elast} and superelastic ϵ_{SE} deformation, together with residual plastic ϵ_{plast} deformation on the maximum indentation depth h_{max} .

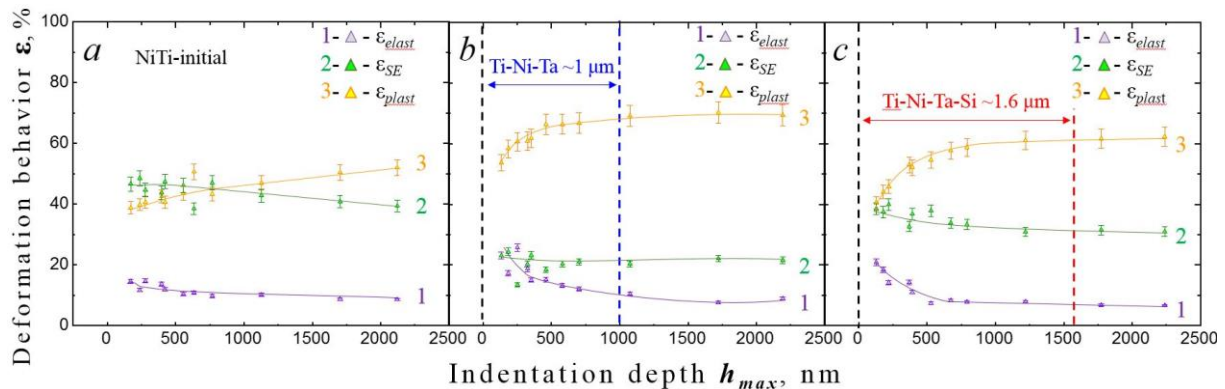


Figure 3. Dependences of the deformation behavior (elastic deformation ϵ_{elast} – curve 1; superelastic deformation ϵ_{SE} – curve 2; plastic deformation ϵ_{plast} – curve 3) for NiTi-initial (a), [Ti-Ni-Ta]SA (b) and [Ti-Ni-Ta-Si]SA (c) on the maximum indentation depth h_{max} . The dotted lines show the boundaries of synthesized SAs according to [5]

For the NiTi-initial, the ϵ_{elast} does not depend on the loading conditions and remains constant at $\sim 10\%$ over the entire analyzed depth (figure 3a, curve 1). In the [Ti-Ni-Ta]SA and [Ti-Ni-Ta-Si]SA near the surface at a depth of ~ 200 nm thickness, the ϵ_{elast} are $\sim 20\%$ (curve 1, figure 3b and c, respectively). Within the layers of both types of SAs at a depth of more than ~ 200 nm thickness, the values of ϵ_{elast} decrease to $\sim 10\%$. In the underlying layers (at a depth of more than ~ 1 μm), the values of ϵ_{elast} are constant.

The values of ϵ_{SE} (figure 3, curves 2) linearly decrease with increasing indentation depth: from ~ 45 up to $\sim 38\%$ in the NiTi-initial (figure 3a), from ~ 40 up to $\sim 35\%$ in the [Ti-Ni-Ta-Si]SA (figure 3c). In the [Ti-Ni-Ta]SA (figure 3b), the ϵ_{SE} takes a constant value ($\sim 22\%$).

In the NiTi-initial, the value of ϵ_{plast} (figure 3a, curve 3) over the entire indentation depth is described by a linearly increasing dependence (from ~ 35 up to $\sim 52\%$). Within the layers of both types of SAs, increases of the values of ϵ_{plast} from ~ 52 up to $\sim 65\%$ (figure 3b, curve 3) and from ~ 40 up to $\sim 60\%$ (figure 3c, curve 3), for [Ti-Ni-Ta]SA and [Ti-Ni-Ta-Si]SA, respectively, are observed at depths more than ~ 200 nm thickness. The ϵ_{plast} almost does not change at higher loads on the indenter (at a depth of ~ 2 μm thickness).

4. Conclusions

Based on the results of studies on topographical parameters and mechanical properties of the surface layers of multicomponent systems [[Ti-Ni-Ta]SA/NiTi-substrate] and [[Ti-Ni-Ta-Si]SA/NiTi-substrate], it was found that:

1) the addition of Si₁₀ to the deposited Ti₆₀Ta₃₀Si₁₀ films led to the formation of [Ti-Ni-Ta-Si]SA, which has areas with a crater-like microrelief and with smoothed microrelief. Nevertheless, the value of the integral parameter of roughness R_a^{INT} in [Ti-Ni-Ta-Si]SA has a lower value $\sim 0.095 \mu\text{m}$ than in [Ti-Ni-Ta]SA ($R_a^{INT} \approx 0.195 \mu\text{m}$) (for NiTi-initial $R_a^{INT} \approx 0.06 \mu\text{m}$). Thus, the addition of silicon in [Ti-Ni-Ta-Si]SA leads to a decrease in surface roughness of SA;

2) the presence of [Ti-Ni-Ta]SA and [Ti-Ni-Ta-Si]SA on the surface of NiTi alloy leads to an increase of yield strength σ_y in the surface layers of the material, relative to the NiTi-initial. The [Ti-Ni-Ta]SA and [Ti-Ni-Ta-Si]SA are characterized by a gradual decrease of σ_y from ~ 4.2 up to ~ 1.7 GPa and ~ 1.2 GPa, respectively;

3) the evaluation of the deformation behavior (ϵ_{plast} , ϵ_{SE} , ϵ_{elast}) has shown that in [Ti-Ni-Ta]SA and [Ti-Ni-Ta-Si]SA the proportions of ϵ_{elast} do not change concerning NiTi-initial ($\sim 10\%$). At the local deformation of surface layers of the [SA/NiTi-substrate] systems, due to the increase of ϵ_{plast} , there was a decrease of ϵ_{SE} up to ~ 22 and $\sim 35\%$ in [Ti-Ni-Ta]SA and [Ti-Ni-Ta-Si]SA, respectively (for NiTi-initial $\epsilon_{SE} \approx 38\%$).

Acknowledgments

The used scientific equipment is a part of the Center for the collective use «Nanotech» (ISPMS SB RAS, Tomsk, Russia) and the Center for collective use at the Research Institute of Nuclear Physics (National Research Tomsk Polytechnic University, Tomsk, Russia).

The reported study was funded by Russian Foundation for Basic Research according to the research project No 20-33-90034.

References

- [1] *Shape Memory Alloys: Modeling and Engineering Applications* ed Dimitris C Lagoudas (Chemistry and Materials Science: Springer) 2008
- [2] *Surface Modification and Alloying: by Laser, Ion, and Electron Beams* ed Poate J M, Foti G, Jacobson D C (New York: Plenum Press) 1983
- [3] Markov A B, Mikov A V, Ozur G E, Padei A G 2011 *Instruments and Experimental Techniques* **54(6)** 862–866
- [4] Markov A, Yakovlev E, Shepel D, Bestetti M 2019 *Results Phys.* **12** 1915–1924
- [5] D'yachenko F A, Meisner L L, Shugurov A R, Neiman A A, Semin V O, Atovullaeva A A 2021 *Technical Physics* **66(1)** 46–52
- [6] Yakovlev E V, Markov A B, Shepel D A, Petrov V I, Neiman A A 2021 *Russ. Phys. J.* **63(10)** 1804–1809
- [7] Dao M, Chollacoop N, Van Vliet K J, Venkatesh T A, Suresh S 2001 *Acta mater.* **49(19)** 3899–3918
- [8] F A D'yachenko *et al* 2019 *IOP Conf. Ser.: Mater. Sci. Eng.* **597** 012044